

Mechanism of Action and *In Vivo* Efficacy of a Human-Derived Antibody against *Staphylococcus aureus* α -Hemolysin

Davide Foletti[†], Pavel Strop[†], Lee Shaughnessy, Adela Hasa-Moreno, Meritxell Galindo Casas, Marcella Russell, Christine Bee, Si Wu, Amber Pham, Zhilan Zeng, Jaume Pons, Arvind Rajpal and Dave Shelton

Rinat Laboratories, Pfizer Inc., 230 East Grand Avenue, South San Francisco, CA 94080, USA

Correspondence to Davide Foletti: davide.foletti@pfizer.com.

<http://dx.doi.org/10.1016/j.jmb.2013.02.008>

Edited by J. Bowie

Abstract

The emergence and spread of multi-drug-resistant strains of *Staphylococcus aureus* in hospitals and in the community emphasize the urgency for the development of novel therapeutic interventions. Our approach was to evaluate the potential of harnessing the human immune system to guide the development of novel therapeutics. We explored the role of preexisting antibodies against *S. aureus* α -hemolysin in the serum of human individuals by isolating and characterizing one antibody with a remarkably high affinity to α -hemolysin. The antibody provided protection in *S. aureus* pneumonia, skin, and bacteremia mouse models of infection and also showed therapeutic efficacy when dosed up to 18 h post-infection in the pneumonia model. Additionally, in pneumonia and bacteremia animal models, the therapeutic efficacy of the α -hemolysin antibody appeared additive to the antibiotic linezolid. To better understand the mechanism of action of this isolated antibody, we solved the crystal structure of the α -hemolysin:antibody complex. To our knowledge, this is the first report of the crystal structure of the α -hemolysin monomer. The structure of the complex shows that the antibody binds α -hemolysin between the cap and the rim domains. In combination with biochemical data, the structure suggests that the antibody neutralizes the activity of the toxin by preventing binding to the plasma membrane of susceptible host cells. The data presented here suggest that protective antibodies directed against *S. aureus* molecules exist in some individuals and that such antibodies have a therapeutic potential either alone or in combination with antibiotics.

© 2013 Elsevier Ltd. All rights reserved.

Introduction

Staphylococcus aureus is a versatile pathogen and a common cause of nosocomial and community-acquired infections. While the majority of *S. aureus* infections manifest as skin and soft tissue infections (SSTIs), the pathogen can also cause more invasive and life-threatening diseases such as sepsis, endocarditis, and pneumonia.¹ The emergence and spread, in hospitals and the community, of multi-drug-resistant strains are making therapeutic intervention increasingly difficult and expensive.^{2,3} With only few new antibiotics in development, considerable interest and efforts have been directed towards exploring active and passive immune-mediated therapeutic approaches to prevent and treat staphylococcal infections.^{4,5}

At the same time, *S. aureus* is a human commensal and 20–30% of healthy, symptom-free individuals are persistently colonized in the nose and another 30% carry it intermittently.⁶ Although prior infection with *S. aureus* is generally thought not to result in protective immunity, antibodies against a variety of *S. aureus* molecules have been detected in human blood of healthy donors and in infected individuals and their possible protective role remains a matter of debate (reviewed in Ref. 7).

S. aureus has a formidable arsenal of virulence factors that represent potential targets for both active and passive immunotherapy.⁸ α -Hemolysin is among the first characterized and best-studied pore-forming cytotoxins of *S. aureus* (reviewed in Ref. 9). At low concentrations, the toxin induces pro-inflammatory mediators (reviewed in Ref. 10) and

promotes breach of the epithelial barrier, at least in part by binding and activating the zinc-dependent metalloprotease ADAM10, resulting in E-cadherin cleavage and disruption of intercellular adherens junctions.^{11–13} At high concentrations, α -hemolysin forms a complex that creates a pore on susceptible host cell plasma membranes leading to a disruption of ion gradients, loss of membrane integrity, and direct lysis. The crystal structure of the fully assembled α -hemolysin pore complex¹⁴ revealed that seven α -hemolysin monomers assemble on the membrane to form the lytic pore with each monomer donating two β -strands that make up the membrane-spanning β -barrel.

The critical role of α -hemolysin as a virulence factor has been demonstrated in multiple animal models of staphylococcal diseases including pneumonia,^{15,16} dermonecrotic skin infection,¹⁷ corneal infection,¹⁸ and intraperitoneal infection.¹⁹ Active (with toxoids or non-hemolytic variants) and passive immunization studies (with antibodies derived from mice and rabbits) in a number of animal models have shown protective efficacy, highlighting the importance of this toxin and its potential as a target for immunotherapy.^{17,20–24}

To further explore the potential functional significance of preexisting antibodies in the serum of

human individuals, and to identify potentially therapeutic α -hemolysin antibodies against *S. aureus* infection, we isolated an α -hemolysin antibody from human donors and characterized its properties.

Results

Human serum contains antibodies with functional blocking activity against α -hemolysin

To determine if there is a correlation between the titer and functional activity of preexisting antibodies against α -hemolysin, we analyzed the serum of 90 healthy human donors. We observed a large interindividual variability both in the titer of α -hemolysin-specific antibodies and in the ability to block α -hemolysin lysis (Fig. 1a). Although there is a statistically significant correlation between the ELISA titer and the functional blocking activity of α -hemolysin antibodies (i.e., higher titer providing better blocking activity), it is clear that individuals with similar titers can have blocking activity that varies over 2 orders of magnitude. This suggests that not only do different individuals have different levels of

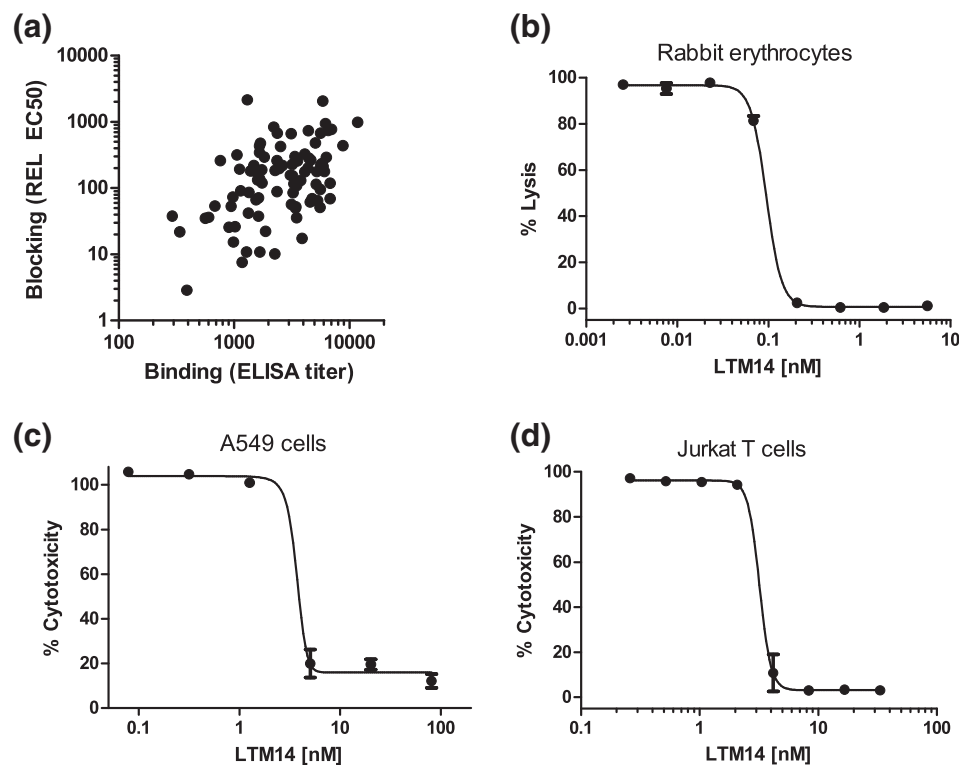


Fig. 1. Titer and blocking activity of antibodies against α -hemolysin in human serum samples and *in vitro* neutralizing activity of LTM14. (a) The ELISA titer of antibodies against α -hemolysin for 90 human serum samples correlates with their ability to block the lytic activity of the toxin in the RE lysis assay (REL EC₅₀; Pearson's correlation coefficient $r=0.306$, $p=0.0039$). LTM14 dose-dependently blocks (b) the lytic activity of α -hemolysin on REs, (c) the cytotoxic activity of α -hemolysin on A549 cells, and (d) the cytotoxic activity of α -hemolysin on Jurkat T cells.

preexisting antibodies against α -hemolysin, but more importantly that the neutralizing capacity of these preexisting antibodies varies considerably.

Isolation of a high-affinity α -hemolysin blocking antibody from a human-derived phage display library

We isolated antibodies against α -hemolysin from a single-chain variable fragment (scFv) phage library built from human donors.²⁵ Sequence analysis of clones with good binding and functional blocking in the rabbit erythrocyte (RE) lysis assay revealed the presence of one dominant heavy-chain variable domain sequence (VH) family paired up with a number of different and apparently unrelated light-chain variable domain sequences (VL) (data not shown).

One representative clone in this family, LTM14, was converted to a full IgG and further characterized. The *in vitro* affinity of LTM14 for α -hemolysin was determined via the kinetic exclusion assay (KinExA), a method that allows quantification of high-affinity antigen/antibody interactions in solution.²⁶ The equilibrium dissociation constant (K_d value) was determined to be 1.7 pM, a remarkably high affinity for an antibody derived from a phage display library. LTM14 can dose-dependently block the lytic activity of α -hemolysin in the RE assay (Fig. 1b) as well as the α -hemolysin-induced cytotoxicity on the lung epithelial cell line A549 cells and on Jurkat T cells (Fig. 1c and d, respectively).

Structure of α -hemolysin monomer in complex with LTM14

To characterize the neutralizing mechanism of LTM14, we determined the co-crystal structure of the LTM14 Fab in complex with recombinant *S. aureus* α -hemolysin H35L (a previously described nontoxic mutant²⁷). The structure revealed that LTM14 binds to a nonlinear, three-dimensional epitope between the cap and rim domains of α -hemolysin (Fig. 2a). The asymmetric unit contains a single monomer of α -hemolysin bound to the LTM14 antibody. The structure of α -hemolysin in its heptameric form¹⁴ and structures of *S. aureus* leukocidins and γ -hemolysin in monomeric,^{28–30} heterodimeric,³¹ and octameric³² forms were published previously. To our knowledge, the structure presented here is the first structure of *S. aureus* α -hemolysin in its monomeric form. Superposition of the α -hemolysin monomer determined in this study with a monomer taken out of the heptameric structure is shown in Fig. 2b. Apart from the large differences in the stem and latch regions of α -hemolysin, which are expected due to their involvement in the heptamer formation, the structure of the α -hemolysin monomer is nearly identical with the monomer from the

heptameric structure and superposes with an RMSD of 0.6 Å for 213 C $^\alpha$ atoms.

Comparison of α -hemolysin and LukF monomers

A superposition of the α -hemolysin monomer with the LukF monomer [Protein Data Bank (PDB) ID: 1PVL]²⁹ is shown in Fig. 2c. Despite the low sequence identity at the amino acid level (31.7%) between LukF and α -hemolysin, the structures of the monomers are remarkably similar with an RMSD of 1.0 Å for 203 C $^\alpha$ atoms. Due to the moderate resolution of the α -hemolysin:LTM14 complex (3.35 Å), it is difficult to analyze the structures in atomic detail; however, the overall conformations of the triangle, stem, and latch regions can still be analyzed. Both the triangle and stem regions of the α -hemolysin monomer (triangle residues 102–111 and 148–152, stem residues 112–127) adopt a conformation very similar to the monomeric form of LukF. Stem residues 128–131 and 141–145 deviate from LukF, while residues 133–140 are disordered as was observed in the LukF structure. The latch in the monomer of α -hemolysin also adopts a conformation similar to that of LukF and is folded into an N-terminal β -strand. Residues 1–9 appear more disordered than in the LukF structure and could not be unambiguously built into the electron density. This could be partly due to the longer C-terminus of LukF, which extends β -strand 16 and can potentially stabilize more residues in the monomeric conformation of the latch.

LTM14 Fab: α -hemolysin interaction

The crystal structure shows that the interaction between LTM14 and α -hemolysin is mediated mainly by the heavy chain (Fig. 2d), a finding consistent with the panning results where one dominant VH family was observed paired with several unrelated VLs. The surface area of α -hemolysin buried by LTM14 Fab is approximately 965 Å², while the surface area of LTM14 buried by α -hemolysin is approximately 881 Å². The heavy chain contributes 90.1% (794 Å²) of buried surface area while the light chain contributes only 9.9% (87 Å²). α -Hemolysin binds mainly to a cleft that is created by the heavy-chain CDR1 (complementarity-determining region 1) and CDR2 loops on one side and CDR3 on the opposite side (Fig. 2e).

Interestingly, the epitope of LTM14 is centered on α -hemolysin residue R66, which has been implicated in binding to the eukaryotic membrane.³³ Residues that were found in this study to be important for α -hemolysin membrane interaction³³ are shown on the α -hemolysin structure in Fig. 3a (R66, E70, R200, D255, and D276). With the exception of R200, LTM14 binds directly to or right next to these residues, which should prevent α -hemolysin binding to the membrane (Fig. 3a).

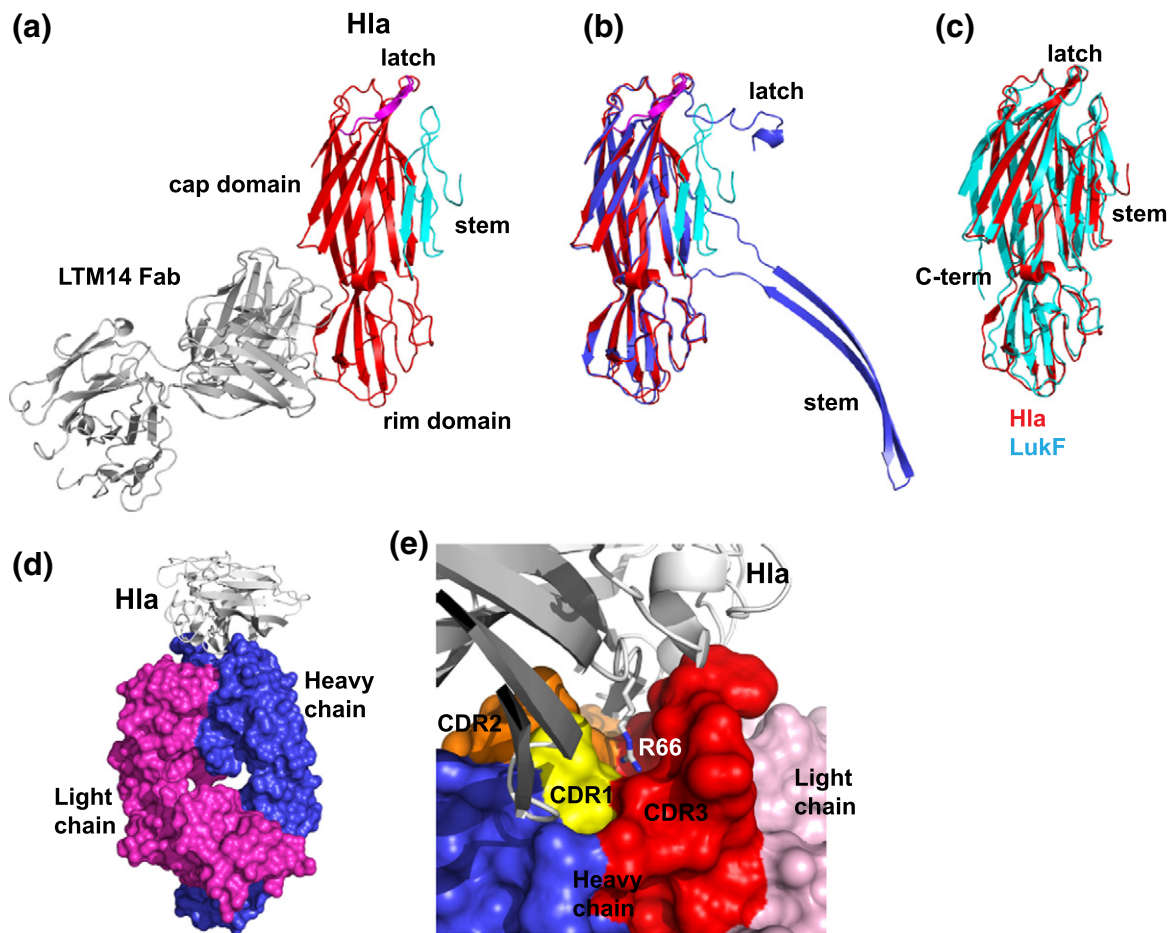


Fig. 2. Crystal structure of the α -hemolysin:LTM14 complex. (a) Ribbon diagram of the α -hemolysin:LTM14 complex. LTM14 Fab is shown in gray; α -hemolysin is shown in red with the latch in magenta and the stem in cyan. (b) Superposition of the α -hemolysin monomer from the α -hemolysin:LTM14 structure (red) with an α -hemolysin monomer, derived from the heptameric structure¹⁴ (blue). (c) Superposition of the α -hemolysin monomer from the α -hemolysin:LTM14 structure (red) with the LukF monomer (cyan). (d) Contribution of the heavy and light chains to α -hemolysin binding. LTM14 Fab is shown in surface representation with the heavy chain shown in blue and the light chain in magenta; α -hemolysin is shown as gray ribbon representation. (e) LTM14 binds α -hemolysin mainly between the cleft created by CDR1 (yellow)/CDR2 (orange) and CDR3 (red) of the heavy chain and is centered on the α -hemolysin R66 residue. The heavy chain of LTM14 is shown in blue apart from the CDRs, the light chain is shown in pink, and α -hemolysin is shown in gray ribbons.

In order to test this hypothesis, we performed α -hemolysin membrane binding experiments in the presence of LTM14. α -Hemolysin, with or without prior incubation with LTM14, was incubated with RE and the association of the toxin with the RE membranes was detected by Western blot. The data show that pre-incubating α -hemolysin with LTM14 completely abolishes binding of the toxin to the RE (Fig. 3b and c). We next tested if LTM14 blocks the interaction of α -hemolysin with its specific membrane receptor ADAM10.^{13,34} Cell-associated metalloprotease activity was measured with a fluorogenic peptide substrate assay in A549 human alveolar epithelial cells stimulated with α -hemolysin. Pre-incubation of α -hemolysin with increasing concentrations of LTM14 blocked the toxin-induced increase in ADAM10 activity (Fig. 3d).

These data strongly suggest that the mechanism through which LTM14 inhibits α -hemolysin function is by preventing the toxin from binding to the membrane directly or through ADAM10.

Based on the previously published structure of the α -hemolysin heptamer, the LTM14 epitope does not get occluded upon α -hemolysin heptamer formation and could be potentially available for LTM14 binding. It might be possible for seven LTM14 Fabs to bind to the α -hemolysin heptamer in solution (Fig. 3e); however, since the heptamer is naturally formed on the membrane, the Fabs would have to partially insert into the membrane to achieve such binding (Fig. 3f). Because this process would be highly energetically unfavorable and because full-length IgGs are even larger than the shown Fabs, we presume that LTM14

is unlikely to be able to bind to the fully assembled membrane-bound heptameric pore complex.

In vivo efficacy in a pneumonia model

Methicillin-resistant *S. aureus* (MRSA) accounts for 10–40% of health-care-associated, hospital-

acquired, and ventilator-associated pneumonia cases with mortality rates as high as 50%.^{35,36} Therefore, we tested the efficacy of LTM14 in an intranasal murine model of *S. aureus* pneumonia (Fig. 4). In a prophylactic protocol (antibody dosed 24 h prior to the bacterial challenge with USA300 LAC), LTM14 afforded near-complete protection with

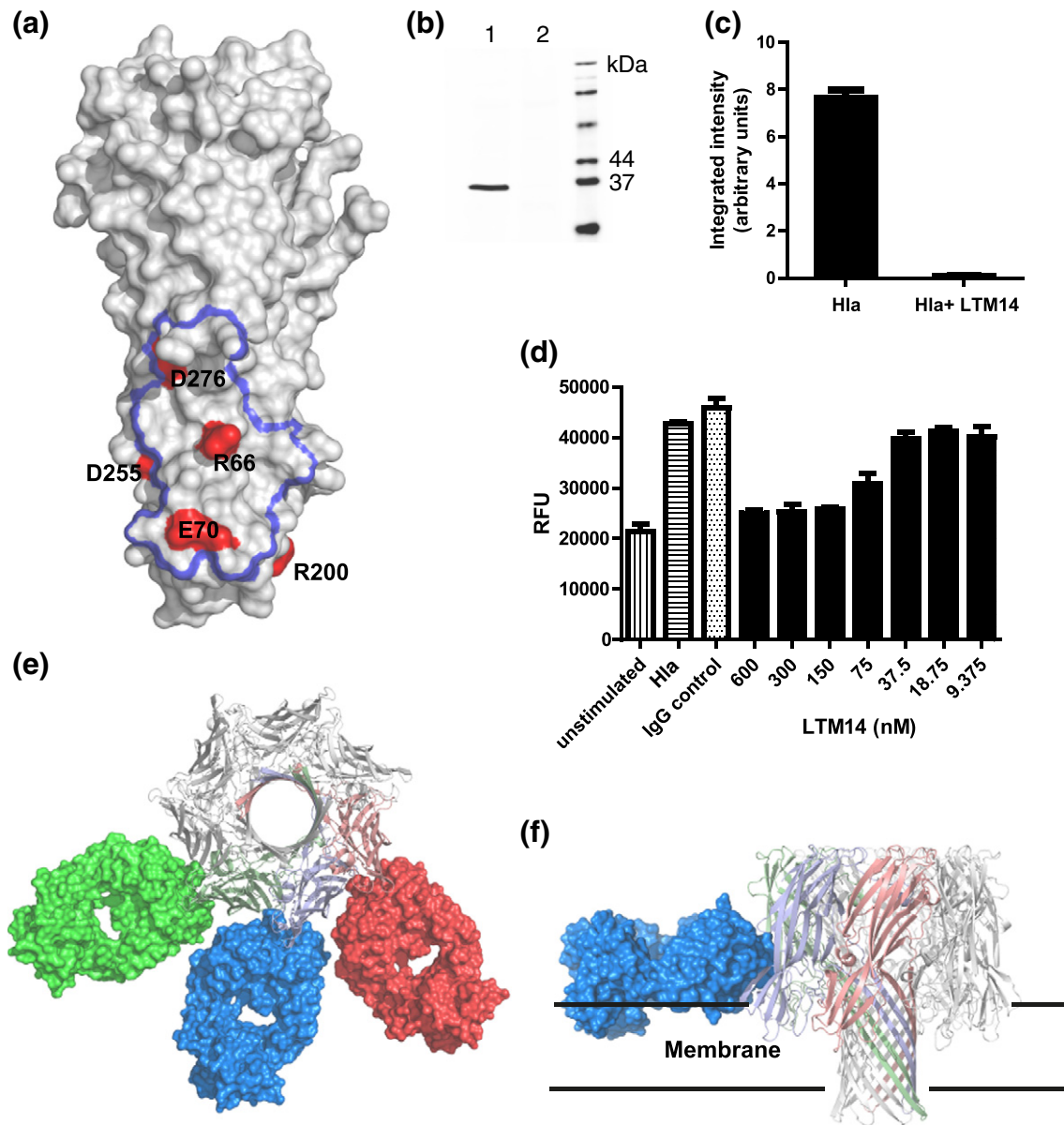


Fig. 3. Mechanism of LTM14 antibody blocking activity. (a) Surface representation of the α -hemolysin monomer, with residues previously found to contribute to membrane binding shown in red. The epitope outline of the LTM14 antibody is shown in blue. Pre-incubation of α -hemolysin with LTM14 abolishes binding of the toxin to RES. (b) Example of Western blot results; α -hemolysin without prior incubation with LTM14 is detected on the erythrocyte membrane (lane 1), while pre-incubation with the antibody abolishes binding (lane 2). (c) Bar graph representation of the α -hemolysin band intensity for three independent experiments (average and SEM). (d) Pre-incubation of α -hemolysin with LTM14 blocks the toxin-dependent activation of ADAM10 on A549 cells (one of three independent experiments). (e) Model of the Fab interaction with the α -hemolysin heptamer showing that the Fab fragment could potentially bind the heptamer in solution. Only three Fabs are shown for clarity. (f) Side view of a model showing how the Fab fragment would be positioned relative to the membrane.

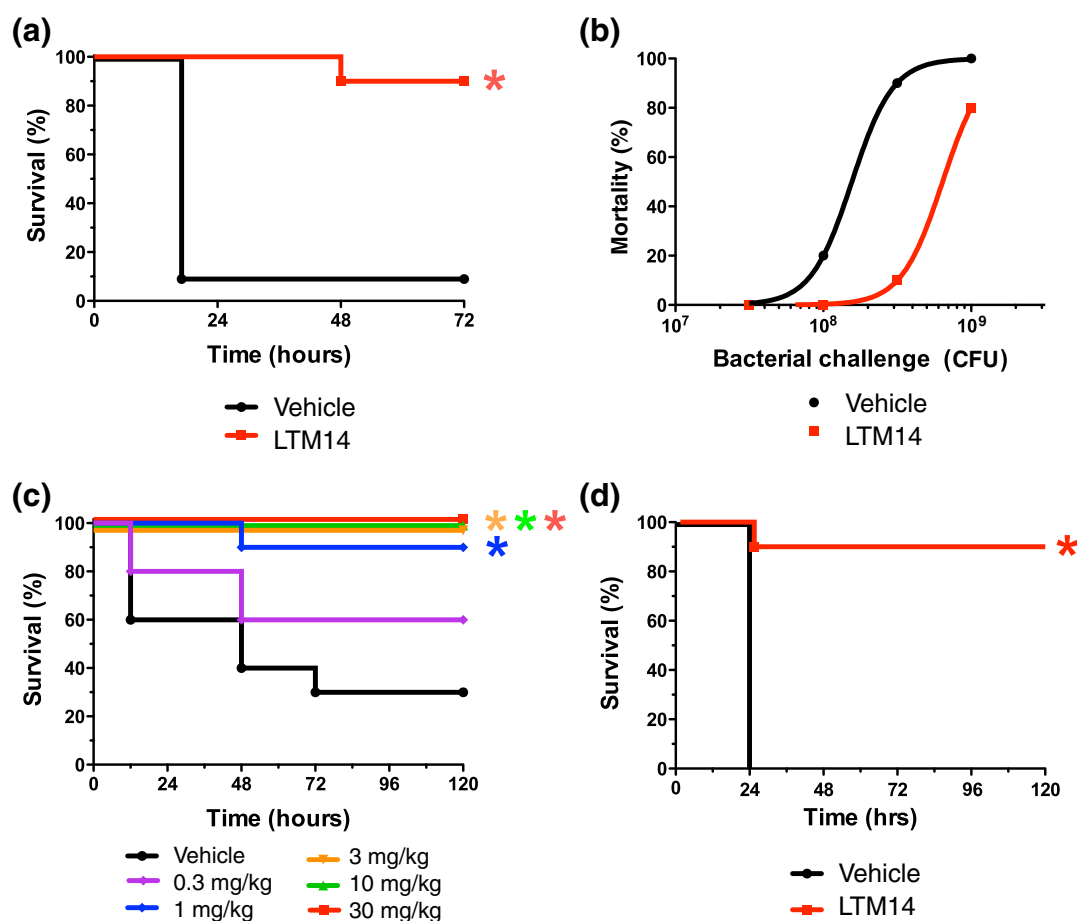


Fig. 4. *In vivo* efficacy of LTM14 in a mouse model of *S. aureus* pneumonia, prophylactic antibody administration. (a) Survival curves for groups of mice dosed with LTM14 (30 mg/kg ip) or vehicle before intranasal challenge with 3.2×10^8 CFU of *S. aureus* USA300 LAC ($n = 10$ mice per group, $*p < 0.001$ compared to vehicle, log-rank test). (b) Dosing of LTM14 (30 mg/kg) increases the LD_{50} of the bacterial challenge ($n = 10$ mice per group, intranasal challenges of 3×10^7 , 1×10^8 , 3×10^8 , and 1×10^9 CFU of *S. aureus* USA300 LAC). (c) Survival curves for mice dosed with decreasing amounts of LTM14 or vehicle and challenged with 3×10^8 CFU of *S. aureus* USA300 LAC ($n = 10$ mice per group, $*p < 0.05$ compared to vehicle, log-rank test). (d) Survival curves for groups of mice dosed with LTM14 (30 mg/kg ip) or vehicle before intranasal challenge with 8×10^8 CFU of *S. aureus* PFESA0140 ($n = 10$ mice per group, $*p < 0.001$ compared to vehicle, log-rank test). All animals were dosed 24 h prior to infection.

90% survival rates at 72 h while the survival rate in the vehicle group was reduced to 10% by 24 h (Fig. 4a). LTM14 also increased survival rates at lower [1×10^8 colony-forming units (CFU)] and higher (1×10^9 CFU) inoculi, effectively shifting the LD_{50} of the bacterial challenge by over fourfold (Fig. 4b). In a dose-response study, LTM14 provided full protection at 3 mg/kg and approximately 50% protection at 0.3 mg/kg (Fig. 4c). LTM14 was also tested in the intranasal infection model with a methicillin-sensitive clinical isolate *S. aureus* strain (Pfizer PFSA0140) and proved to be equally efficacious (Fig. 4d).

Next, we tested the efficacy of LTM14 in a therapeutic dosing protocol to assess the ability of the antibody to increase survival rates when administered after the bacterial challenge (Fig. 5a).

In the pneumonia model, mice typically show prominent signs of disease by 12 to 18 h, attesting to the quick advancement of the infection. Full survival was observed with both LTM14 and linezolid treatments administered up to 12 h after inoculation. Even when dosed 18 h after challenge, both treatments afforded 40–50% survival.

To determine if there is an increased benefit of combination treatment, we co-administered LTM14 and linezolid prior to a USA300 LAC challenge (Fig. 5b). We utilized a bacterial inoculum that would result in approximately 50% survival with either treatment alone and observed a statistically significant increase in the survival rate to 90% with the combination of LTM14 and linezolid. Together, these data demonstrate that LTM14 not only was capable of protecting mice from a lethal pulmonary challenge

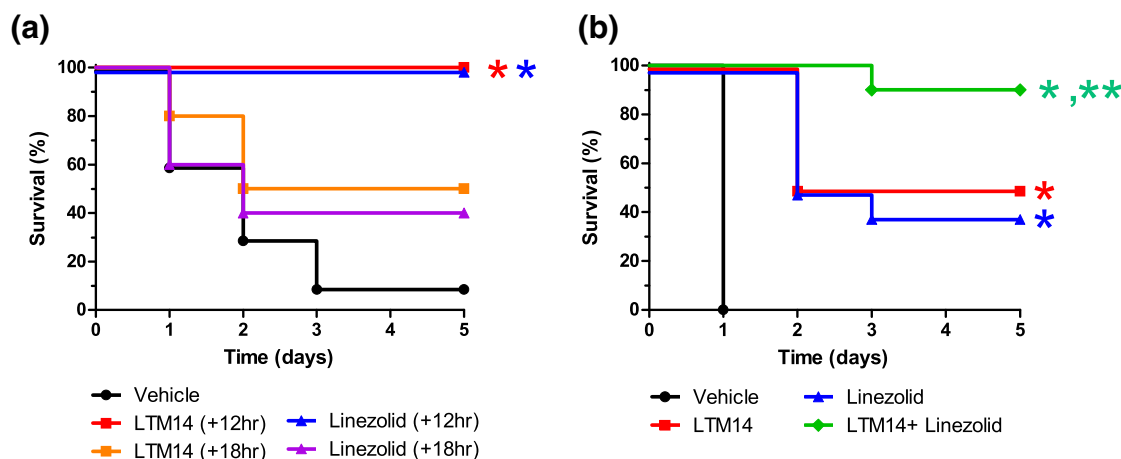


Fig. 5. *In vivo* efficacy of LTM14 in a mouse model of *S. aureus* pneumonia, therapeutic antibody administration and combination with linezolid. (a) Survival curves for groups of mice dosed with either 30 mg/kg LTM14 or 12 mg/kg linezolid 12 and 18 h after intranasal challenge with 5×10^8 CFU of *S. aureus* USA300 LAC ($n=10$ mice per group, * $p < 0.0001$ compared to vehicle, log-rank test). (b) Survival curves for groups of mice dosed with 30 mg/kg LTM14 or 12 mg/kg linezolid individually or in combination 24 h before intranasal challenge with 1×10^9 CFU of *S. aureus* USA300 LAC ($n=10$ mice per group; * $p < 0.0001$ compared to vehicle, ** $p < 0.05$ for the combination compared to the individual treatments, log-rank test).

of *S. aureus* in a prophylactic setting but also could provide improved survival outcome when dosed therapeutically up to 18 h following inoculation of the bacteria. Moreover, the α -hemolysin neutralizing activity of LTM14 and its efficacy in this model were shown to be additive to the activity of the antibiotic linezolid.

***In vivo* efficacy in a skin abscess and dermonecrosis model**

In the past 10–15 years, MRSA USA300 strains have emerged as a predominant cause of SSTIs in the United States.^{37,38} Since a role of α -hemolysin has been previously demonstrated in both mouse and rabbit models of *S. aureus* SSTIs, we compared LTM14 to linezolid in a mouse model of skin abscess and dermonecrosis.^{17,39} Upon intradermal challenge with *S. aureus* USA300 LAC, prophylactic administration of LTM14 effectively reduced the size of the abscess at all time points in the study and nearly abolished the occurrence of dermonecrosis compared to vehicle (Fig. 6a). LTM14 also significantly reduced bacterial burden, albeit not as much as the double dose of linezolid (Fig. 6b). These data build upon the previously published results with polyclonal antibodies¹⁷ and demonstrates the potential use of α -hemolysin neutralizing monoclonal antibodies (mAbs) in SSTIs.

***In vivo* efficacy in a bacteremia model**

α -Hemolysin has previously been shown to be important in staphylococcal bloodstream and sepsis models.¹² Since bacteremia and sepsis are respon-

sible for approximately 80% of all invasive forms of MRSA disease,² we tested LTM14 activity in a mouse model of *S. aureus* bacteremia. When the animals received a challenge of *S. aureus* USA300 LAC, a single prophylactic dose of LTM14 more than doubled the survival rate (Fig. 6c). Additionally, LTM14 was equally efficacious in increasing survival rates with a methicillin-sensitive clinical isolate *S. aureus* strain (Pfizer PFSA0158, data not shown). We next compared the efficacy of LTM14 and linezolid individually or in combination (Fig. 6d). Upon challenge with *S. aureus* USA300 LAC, the combination treatment was more efficacious than either treatment alone. To our knowledge, the data shown here represent the first demonstration of efficacy of an α -hemolysin neutralizing mAb in an intravenous *S. aureus* infection model.

Discussion

S. aureus is a major human pathogen that can cause life-threatening invasive infections such as bacteremia, pneumonia, and endocarditis.¹ *S. aureus* infections can be difficult to treat because of rising antibiotic resistance, and while once mainly associated with nosocomial settings, *S. aureus* infections have more recently spread into the community. At the same time, *S. aureus* is a common human commensal organism that persistently or intermittently colonizes the nares and skin of 30–50% of healthy adults.⁶ Antibodies against staphylococcal proteins have been detected in human serum of healthy individuals, carriers, and infected patients, but their possible protective role against infection

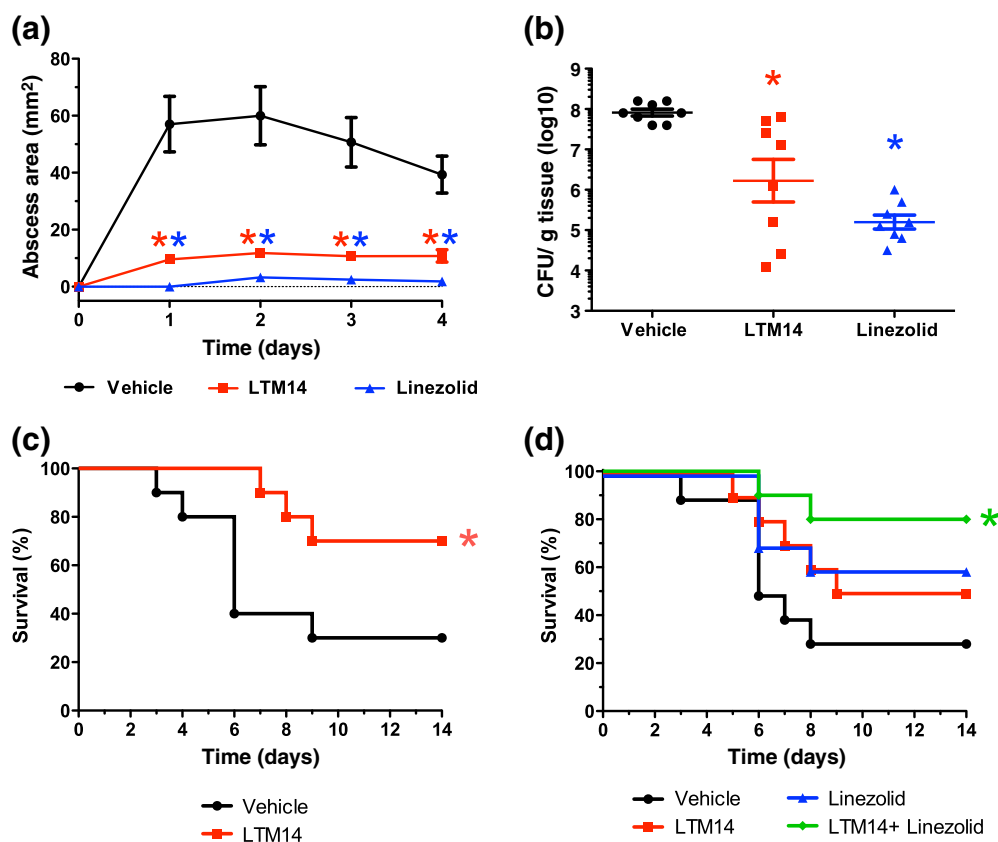


Fig. 6. *In vivo* efficacy of LTM14 in mouse models of skin abscess/dermonecrosis and bacteremia. (a) Groups of mice received a single dose of 50 mg/kg LTM14 24 h before challenge or two doses of 50 mg/kg linezolid, immediately following challenge and again at 24 h after challenge. All groups were delivered an intradermal injection of 1×10^7 CFU of *S. aureus* USA300 LAC. The abscess area was measured daily. Results are the mean value \pm standard error of the mean for all groups ($n = 11$ mice per group, $*p < 0.0001$ compared to vehicle, two-way ANOVA and Bonferroni's post test). (b) Bacterial burden in the infected area excised at day 4 ($n = 8$ mice per group, $*p < 0.05$ compared to vehicle, ANOVA and Dunnett's post test). (c) Survival curves for groups of mice dosed with LTM14 (30 mg/kg ip) or vehicle 24 h before intravenous challenge with 1×10^7 CFU of *S. aureus* USA300 LAC ($n = 10$ mice per group, $*p < 0.05$ compared to vehicle, log-rank test). (d) Survival curves for groups of mice dosed with 30 mg/kg LTM14 or 6.25 mg/kg linezolid individually or in combination 24 h before intravenous challenge with 2×10^7 CFU of *S. aureus* USA300 LAC ($n = 10$ mice per group, $*p < 0.05$ for the combination of LTM14+linezolid compared to vehicle).

continues to remain a matter of debate.^{7,40–43} For example, a recent publication has shown that higher levels of preexisting antibodies against *S. aureus* toxins (including α -hemolysin) are associated with a lower risk of sepsis in patients with *S. aureus* bacteremia,⁴⁴ while another group has shown that naturally occurring antibodies against clumping factor A, another established staphylococcal virulence factor, are not functional and unable to prevent binding to the cognate host target fibrinogen.⁴⁵

To further explore the role of preexisting antibodies against *S. aureus* molecules, we isolated and characterized LTM14, an antibody against α -hemolysin from a human donor library. LTM14 binds α -hemolysin with very high affinity (1.7 pM), which is unusual for an antibody derived from a phage display library. The high binding affinity, the presence of a dominant family of related VH clones in the library

panning output, and the fact that there are a number of framework mutations that deviate from the germline sequence strongly suggest that the heavy chain of LTM14 represents the heavy chain of an α -hemolysin-specific antibody present in one of the library donors and that this antibody had undergone significant *in vivo* affinity maturation in that individual.

LTM14 showed potent α -hemolysin neutralizing activity *in vitro*. To better understand its mechanism of action, we solved the crystal structure of the antibody Fab in complex with recombinant α -hemolysin. The antibody binding site is primarily contributed by the heavy chain (90.1% of the buried surface area) and the epitope is located between the cap and rim domains of α -hemolysin with the heavy-chain CDR1 and CDR2 loops on one side and the CDR3 loop on the opposite side forming a snug binding pocket for the side chain of residue R66 of

α -hemolysin. This provides a mechanistic explanation for the neutralizing activity of LTM14 as the epitope comprises residues previously shown to be important for binding to target membranes.³³

Interestingly, the proposed mechanism of action of LTM14 (inhibition of α -hemolysin binding to the membrane and blocking its interaction with ADAM10) differs significantly from the inhibition of heptamer formation reported for previously described mouse antibodies.^{22,24} It will be interesting to characterize other human antibodies against α -hemolysin and determine their epitopes to ascertain if there are differences in protective capacity based on the location of the epitope and the mechanism of action.

LTM14 showed strong *in vivo* efficacy when dosed prophylactically in mouse models of pneumonia, skin abscess and dermonecrosis, and bacteremia. In the lung model, the antibody was able to provide 90–100% protection compared to near-complete mortality in the control group. In the skin and dermonecrosis model, our α -hemolysin neutralizing antibody effectively reduced the size of the abscess, nearly abolished the occurrence of dermonecrosis, and significantly reduced bacterial burden compared to control. In the bacteremia model, LTM14 more than doubled the survival rate compared to the control group. While mouse antibodies and rabbit antisera directed against α -hemolysin have previously been shown to be efficacious in animal models of staphylococcal infection,^{17,21–24} to our knowledge, this is the first report of a human-derived mAb with efficacy across a panel of *S. aureus* mouse models of disease. LTM14 appears to be more efficacious than the previously described mouse mAbs against α -hemolysin. These mAbs were able to provide a significant survival benefit from 24-h mortality, but the effect was not durable and late mortality (72 h) was similar to that observed in the control.²² The superior efficacy of LTM14 may be due to slight differences in the animal model, or some combination of its stronger affinity for α -hemolysin, its binding epitope on the toxin, and its mechanism of neutralization.

Our results demonstrating efficacy when LTM14 was administered therapeutically in the mouse lung infection model have the potential for far-reaching clinical impact considering the high morbidity and mortality associated with *S. aureus* nosocomial pneumonia, for example, in intensive care unit patients that are on a ventilator.^{35,46} Additionally, LTM14 showed increased efficacy in combination with the antibiotic linezolid. This is significant because in a therapeutic setting in humans, passive immune therapy is most likely going to be administered in combination with the most appropriate antibiotic.

Taken together, these results indicate that LTM14 shows promising therapeutic potential and it remains to be seen whether the efficacy of LTM14 will

translate to a clinical setting. Our data show that potent neutralizing antibodies against α -hemolysin, and possibly against other staphylococcal virulence factors, can be found in humans and support their development as therapeutics for this dangerous human pathogen.

Materials and Methods

Ethics statement

Human serum samples were received from Bioreclamation (Westbury, NY). All serum samples were from a Food and Drug Administration-licensed and -inspected donor center in the United States. Blood samples were collected from paid and consented donors with institutional review board approval.

All animal studies were conducted at internationally accredited facilities of the Association for Assessment and Accreditation of Laboratory Animal Care International. Studies at TransPharm Preclinical Solutions (Jackson, MI) were carried out in compliance with all the laws, regulations, and guidelines of the National Institutes of Health and with the approval of the TransPharm Preclinical Solutions Institution Animal Care and Use Committee. For studies carried out at Rinat Laboratories, the study protocols were reviewed and approved by the Institution Animal Care and Use Committee in adherence to the U.S. animal welfare act.

Library panning

A human scFv phage library²⁵ was used to select antibodies that specifically bind α -hemolysin from *S. aureus* according to previously published methods.⁴⁷ Briefly, 500 nM biotinylated α -hemolysin (Calbiochem) was serially incubated with the phage library at room temperature (RT) for 1 h and streptavidin magnetic beads (Dynabeads M-280 from Invitrogen) for 30 min. After washing, the bound phage antibodies were eluted with trypsin (50 mg/ml) for 5 min at 37 °C. The eluted phages were amplified in TG1 cells and used for the next rounds of selection with 250 nM biotinylated α -hemolysin. A total of three rounds of panning were performed. scFvs were initially screened for their ability to bind α -hemolysin by ELISA and block the lytic activity of the toxin on RE using cell lysates. Purified scFvs from positive clones were retested, ranked by ELISA and RE lysis assay and sequenced leading to the selection of a clone that was converted to a full IgG format; this mAb was named LTM14.

Protein purification

Recombinant LTM14 Fab was produced by transiently transfecting HEK293 cells using Lipofectamine™ (Invitrogen) following the manufacturer's instructions. LTM14 Fab was purified from conditioned media using a Ni column (Qiagen) using standard techniques. His-tagged α -hemolysin H35L mutant was expressed in *Escherichia coli* and purified using Ni column (Qiagen) using standard techniques. The polyhistidine tag was cleaved with human

alpha-thrombin (Haematologic Technologies Inc.), and α -hemolysin was further purified by SourceS ion-exchange chromatography. LTM14 Fab was mixed with α -hemolysin in 1.2:1 ratio and purified by size-exclusion chromatography on Sephacryl S300 column (GE Healthcare Life Sciences). The complex in 50 mM 2-(N-morpholino)ethanesulfonic acid, pH 6.0, and 100 mM NaCl was concentrated to 5 mg/ml for crystallization.

Enzyme-linked immunosorbent assay

α -Hemolysin (Calbiochem) was coated on ELISA plates (NUNC Maxisorp) at 5 μ g/ml in phosphate-buffered saline (PBS) at 4 °C overnight. The following day, plates were blocked in PBS, 1% w/v bovine serum albumin, and 0.01% v/v Tween-20 and then incubated with human serum samples at the indicated dilution. A goat anti-human horseradish-peroxidase-conjugated secondary antibody (Jackson Immunoresearch) in combination with the TMB 2-component peroxidase substrate (KPL) was used to develop the reaction.

A549 and Jurkat T-cell cytotoxicity assay, ADAM10 assay

The lung epithelial cell line A549 (CCL-185) and the Jurkat T-cell line clone E6-1 (TIB-152) from the American Type Culture Collection were cultured in a 37 °C, 5% CO₂ incubator in F12-K or RPMI-1640 medium supplemented with 10% fetal bovine serum and 2 mM L-glutamine, respectively. A549 cells were seeded at 2×10^4 cells/well in 96-well plates. The following day, serial dilutions of LTM14 were pre-incubated with 20 nM α -hemolysin in tissue culture medium for 15 min at RT before being added to the A549 cells for incubation for an additional 18 h. Cytotoxicity was measured with the CellTiter96 Aqueous One Solution Cell Proliferation Assay (Promega) according to the manufacturer's recommendations. Serial dilutions of LTM14 were pre-incubated with 15 nM α -hemolysin in tissue culture medium for 15 min at RT and then added to Jurkat T cells at a density of 150,000 cells per well and incubated overnight. The following day, cytotoxicity was measured by FACS on a BD-LSRII instrument using propidium iodide (Calbiochem) according to the manufacturer's recommendations. For the ADAM10 metalloprotease assay, A549 cells were plated at a density of 1.5×10^4 cells/well in 96-well plates. The following day, 300 nM α -hemolysin, with or without prior incubation with serial dilutions of LTM14, was added to the cells and incubated for 60 min. Cells were washed once in 25 mM Tris (pH 8.0) buffer and incubated for 30 min at 37 °C with 10 μ M fluorogenic peptide substrate (Mca-PLAVQ-Dpa-RSSSR-NH₂, R&D Systems). Fluorescence intensity was read on a FlexStation instrument (Molecular Devices) and expressed as relative fluorescence units.

Rabbit erythrocyte lysis assay

Antibody serial dilutions or serum samples were incubated with 0.5 nM (EC₅₀) α -hemolysin at RT for 30 min in a 0.1-ml volume before being added to 0.1 ml of a suspension of 1% RE and incubated at 37 °C for 1 h in a 96-well plate. The plate was subsequently spun at

2400 rpm for 5 min to pellet intact and lysed RE. The absorbance of the supernatant was read at 405 nm to quantify the amount of released hemoglobin as a measure of lysis.

Binding of α -hemolysin to REs

α -Hemolysin can readily and irreversibly bind to RE at 4 °C, but lysis at 4 °C requires significantly higher concentrations of the toxin compared to when the incubation is carried out at RT or 37 °C.⁴⁸ α -Hemolysin (0.5 μ M) was incubated with 2.5 μ M LTM14 for 30 min at RT and added to the pellet obtained from 250 μ l of 10% RE; the cells were resuspended and incubated for 15 min at 4 °C. REs were washed with 4 °C PBS, resuspended in 0.5 ml of PBS and 0.1% bovine serum albumin, and incubated at RT for 1 h. The samples were spun down and the supernatants were removed. To lyse the intact RE and prepare membranes, we subjected samples to three cycles of resuspension in 1 ml of ddH₂O, incubation for 10 min at RT, and centrifugation at 13,000 rpm. The membranes were solubilized in 10 mM Tris-HCl, pH 7.4, 150 mM NaCl, 1% Triton X-100, and 1% sodium deoxycholate. The solubilized samples were reduced, boiled, and separated on a 4–12% SDS-PAGE gel and transferred to nitrocellulose, and the α -hemolysin monomer was detected with a polyclonal antibody (Sigma). Detection and quantitation were performed with a Li-Cor-Odyssey infrared imager.

Affinity measurement by KinExA

A constant concentration of α -hemolysin was titrated with a dilution series of the antibody, the samples were equilibrated, and free α -hemolysin was measured with a KinExA 3000 instrument (Sapidyne Inc., Boise, ID) to determine the binding affinity of LTM14 for α -hemolysin. All samples were analyzed in duplicate, and all steps were performed at RT (20–25 °C). The measured values were fit to a standard bimolecular binding equation to obtain the K_D value of the interaction.

Crystallization, data collection, and refinement

α -Hemolysin:LTM14 complex crystals were grown by the hanging drop method at 25 °C using a precipitant solution containing 1.7 M AmSO₄, 4.25% v/v isopropanol, and 15% v/v glycerol. Oval-shaped crystals appeared in a week and were directly flash frozen in liquid nitrogen. Diffraction data were collected at Advanced Light Source beamline 5.0.2. The crystals belong to the space group $P6_322$ with unit cell dimensions $a=b=130.2$ Å, $c=308.3$ Å, and $\gamma=120^\circ$ and diffracted to 3.35 Å resolution (Table 1). All diffraction data were processed with DENZO and SCALEPACK.⁴⁹ The structure of the α -hemolysin:LTM14 complex was solved by molecular replacement using a monomer from the α -hemolysin heptamer structure with stem and latch regions removed (PDB ID: 7AHL) and a model of LTM14 Fab using PHASER.⁵⁰ Alternate cycles of model building using the program Coot,⁵¹ positional, TLS, and individual restrained thermal factor refinement in REFMAC,⁵² and addition of water molecules reduced the

Table 1. Refinement and model statistics

Space group	$P6_322$
Cell dimensions	
<i>a</i> , <i>b</i> , <i>c</i> (Å)	130.2, 130.1, 308.3
γ (°)	120
Resolution (Å)	30.0–3.35
Measured reflections	137,395
Unique reflections	22,137
R_{merge}	15.2 (55.4)
Completeness (%)	96.3 (91.3)
$I/\sigma(I)$	9.8 (1.8)
Number of protein atoms	5525
R_{cryst}	24.9
R_{free}	29.6
RMSD	
Bonds (Å)	0.008
Angles (°)	1.1
Ramachandran statistics	
Most favored regions (%)	79.2
Additional allowed regions (%)	18.9
Generously allowed regions (%)	1.9
Disallowed regions (%)	0.0

R and R_{free} values to 25.0% and 31.0%, respectively, for all of the reflections.

Epitope identification and buried area calculations

The epitope residues for LTM14 on the α -hemolysin protein were identified by calculating the difference in accessible surface area between the α -hemolysin:LTM14 crystal structure and the α -hemolysin structure alone. α -Hemolysin residues that show buried surface area upon complex formation with LTM14 were defined as being part of the epitope. The solvent-accessible surface of a protein was calculated with the program AREAIMOL.⁵³

Bacterial strains and preparation

S. aureus strains USA300 LAC and PFESA0140 were swabbed onto trypticase soy agar plates supplemented with 5% sheep blood cells (BBL, Becton Dickinson Laboratories, Franklin Lakes, NJ) and grown overnight at 37 °C. Bacteria were cultured in trypticase soy broth (TSB) at 37 °C until the culture arrived at an OD₆₀₀ (optical density at 600 nm) of 0.6, providing a bacterial concentration of approximately 1×10^8 CFU/ml. The culture was centrifuged and the pellet was resuspended in 4 ml of TSB to bring the bacterial concentration to approximately 2.0×10^{10} CFU/ml. This concentrated culture was diluted in TSB to prepare the challenge with the desired CFU per animal.

Lung infection model

Female, 7- to 8-week-old Balb/c mice weighing 19–21 g were obtained from Charles River. *S. aureus* USA300 LAC and PFESA0140 were prepared as described above. Mice were anesthetized with isoflurane and administered an intranasal challenge (0.05 ml) of the bacterial culture. LTM14 (formulated in PBS) or vehicle was administered in a single intraperitoneal dose at the concentration and time indicated using a 0.5-ml dosing volume. The antibiotic

linezolid was formulated at a dosing concentration of 12 mg/kg in an aqueous solution of 5% polyethylene glycol 200 and 0.5% methylcellulose. Linezolid was administered by oral gavage at the time indicated in a single dose using a 0.5-ml dosing volume. Mortality was recorded over a period of 3–5 days following bacterial challenge.

Skin abscess/dermonecrosis model

Female, 7- to 8-week-old Balb/c mice weighing 19–21 g were obtained from Harlan. One day prior to bacterial challenge, mice were anesthetized with isoflurane and hair was removed from the dorsal side (2×2 cm) using the depilatory agent Nair®. LTM14 (50 mg/kg) and vehicle treatment were administered in an intraperitoneal dose 1 day prior to the bacterial challenge. *S. aureus* USA300 LAC were prepared as described above and mice were infected by intradermal injection of bacteria ($\sim 10^7$ CFU in 0.05 ml). Linezolid (50 mg/kg) was administered immediately following the bacterial challenge and again at 24 h post challenge. Mice were monitored daily and progression of abscess formation was tracked by measuring the length and width of the abscess. For days after infection, mice were humanely euthanized by CO₂ asphyxiation and the skin was homogenized and plated for bacterial enumeration.

Bacteremia model

Female, 7- to 8-week-old Balb/c mice weighing 19–21 g were obtained from Charles River. *S. aureus* USA300 LAC were prepared as described above and diluted to $\sim 2 \times 10^7$ CFU in 0.1 ml. Ten animals per group were anesthetized with isoflurane and administered 0.1 ml of bacterial challenge via lateral tail vein injection. The antibody or vehicle treatments were administered in a single intraperitoneal dose 24 h prior to the bacterial challenge using a 0.5-ml dosing volume. The antibiotic linezolid (6.25 mg/kg) was administered at the time of challenge by oral gavage using a 0.5-ml dosing volume. Mortality was recorded over a period of 14 days following bacterial challenge.

Graphic interpretation of the results, nonlinear regression curve fits, EC₅₀ calculations, and statistical analysis were performed using GraphPad Prism v.5.0.

Accession number

The coordinates for the structure have been deposited in the PDB (PDB ID: 4IDJ).

Acknowledgements

We thank Michael Chin, Charles Appah, Ishita Barman, and Colleen Brown for expression and purification of LTM14; Mark Gilbert for assistance with FACS experiments; Wenwu Zhai for generation of the phage display library and Li Mei for assistance with library panning; Janette Sutton and Ariel Pios for assistance with animal work; Yasmina Abdiche and Kevin Lindquist for assistance with biosensor work;

Javier Chaparro-Riggers and Andy Yeung for discussions; and Jody Melton Witt for critical reading of the manuscript. We thank Annaliesa Anderson and Ingrid Scully (Pfizer Vaccine Research) for providing *S. aureus* strains and for help with the bacteremia model and discussions.

Conflict of Interest Statement. All authors were employees and shareholders of Pfizer Inc. at the time the study was conducted.

Received 17 December 2012;

Received in revised form 1 February 2013;

Accepted 7 February 2013

Available online 13 February 2013

Keywords:

crystal structure;
bacterial toxin;
pathogen;
animal model;
therapeutic

Present addresses: L. Shaughnessy, Stratatech Corporation, 505 South Rosa Road, Madison, WI 53719, USA; S. Wu, Roche GlycArt China, Room 205, Building 5, 399 Cai Lun Road, Pudong, Shanghai 201203, People's Republic of China.

†D.F. and P.S. contributed equally to this work.

Abbreviations used:

CDR, complementarity-determining region; CFU, colony-forming units; KinExA, kinetic exclusion assay; mAb, monoclonal antibody; MRSA, methicillin-resistant *Staphylococcus aureus*; PBS, phosphate-buffered saline; PDB, Protein Data Bank; RE, rabbit erythrocyte; RT, room temperature; scFV, single-chain variable fragment; SSTI, skin and soft tissue infection; TSB, trypticase soy broth.

References

- Lowy, F. D. (1998). *Staphylococcus aureus* infections. *N. Engl. J. Med.* **339**, 520–532.
- Klevens, R. M., Morrison, M. A., Nadle, J., Petit, S., Gershman, K. & Ray, S. (2007). Invasive methicillin-resistant *Staphylococcus aureus* infections in the United States. *JAMA*, **298**, 1763–1771.
- Otto, M. (2012). MRSA virulence and spread. *Cell. Microbiol.* **14**, 1513–1521.
- Broughan, J., Anderson, R. & Anderson, A. S. (2011). Strategies for and advances in the development of *Staphylococcus aureus* prophylactic vaccines. *Expert Rev. Vaccines*, **10**, 695–708.
- Otto, M. (2010). Novel targeted immunotherapy approaches for staphylococcal infection. *Expert Opin. Biol. Ther.* **10**, 1049–1059.
- Vandenbergh, M. F. & Verbrugh, H. A. (1999). Carriage of *Staphylococcus aureus*: epidemiology and clinical relevance. *J. Lab. Clin. Med.* **133**, 525–534.
- Holtfreter, S., Kolata, J. & Broker, B. M. (2010). Towards the immune proteome of *Staphylococcus aureus*—the anti-*S. aureus* antibody response. *Int. J. Med. Microbiol.* **300**, 176–192.
- Kobayashi, S. D. & DeLeo, F. R. (2009). An update on community-associated MRSA virulence. *Curr. Opin. Pharmacol.* **9**, 545–551.
- Bhakdi, S. & Trantum-Jensen, J. (1991). Alpha-toxin of *Staphylococcus aureus*. *Microbiol. Rev.* **55**, 733–751.
- Frank, K. M., Zhou, T., Moreno-Vinasco, L., Hollett, B., Garcia, J. G. & Bubeck Wardenburg, J. (2012). Host response signature to *Staphylococcus aureus* alpha-hemolysin implicates pulmonary TH17 response. *Infect. Immun.* **80**, 2161–3169.
- Inoshima, I., Inoshima, N., Wilke, G. A., Powers, M. E., Frank, K. M., Wang, Y. & Bubeck Wardenburg, J. (2011). A *Staphylococcus aureus* pore-forming toxin subverts the activity of ADAM10 to cause lethal infection in mice. *Nat. Med.* **17**, 1310–1314.
- Powers, M. E., Kim, H. K., Wang, Y. & Bubeck Wardenburg, J. (2012). ADAM10 mediates vascular injury induced by *Staphylococcus aureus* alpha-hemolysin. *J. Infect. Dis.* **206**, 352–356.
- Wilke, G. A. & Bubeck Wardenburg, J. (2010). Role of a disintegrin and metalloprotease 10 in *Staphylococcus aureus* alpha-hemolysin-mediated cellular injury. *Proc. Natl Acad. Sci. USA*, **107**, 13473–13478.
- Song, L., Hobaugh, M. R., Shustak, C., Cheley, S., Bayley, H. & Gouaux, J. E. (1996). Structure of staphylococcal alpha-hemolysin, a heptameric transmembrane pore. *Science*, **274**, 1859–1866.
- Bubeck Wardenburg, J., Patel, R. J. & Schneewind, O. (2007). Surface proteins and exotoxins are required for the pathogenesis of *Staphylococcus aureus* pneumonia. *Infect. Immun.* **75**, 1040–1044.
- Bubeck Wardenburg, J., Bae, T., Otto, M., Deleo, F. R. & Schneewind, O. (2007). Poring over pores: alpha-hemolysin and Pantón–Valentine leukocidin in *Staphylococcus aureus* pneumonia. *Nat. Med.* **13**, 1405–1406.
- Kennedy, A. D., Bubeck Wardenburg, J., Gardner, D. J., Long, D., Whitney, A. R., Braughton, K. R. *et al.* (2010). Targeting of alpha-hemolysin by active or passive immunization decreases severity of USA300 skin infection in a mouse model. *J. Infect. Dis.* **202**, 1050–1058.
- O'Callaghan, R. J., Callegan, M. C., Moreau, J. M., Green, L. C., Foster, T. J., Hartford, O. M. *et al.* (1997). Specific roles of alpha-toxin and beta-toxin during *Staphylococcus aureus* corneal infection. *Infect. Immun.* **65**, 1571–1578.
- Patel, A. H., Nowlan, P., Weavers, E. D. & Foster, T. (1987). Virulence of protein A-deficient and alpha-toxin-deficient mutants of *Staphylococcus aureus* isolated by allele replacement. *Infect. Immun.* **55**, 3103–3110.
- Bubeck Wardenburg, J. & Schneewind, O. (2008). Vaccine protection against *Staphylococcus aureus* pneumonia. *J. Exp. Med.* **205**, 287–294.

21. Menzies, B. E. & Kernodle, D. S. (1996). Passive immunization with antiserum to a nontoxic alpha-toxin mutant from *Staphylococcus aureus* is protective in a murine model. *Infect. Immun.* **64**, 1839–1841.
22. Ragle, B. E. & Bubeck Wardenburg, J. (2009). Anti-alpha-hemolysin monoclonal antibodies mediate protection against *Staphylococcus aureus* pneumonia. *Infect. Immun.* **77**, 2712–2718.
23. Spaulding, A. R., Lin, Y. C., Merriman, J. A., Brosnahan, A. J., Peterson, M. L. & Schlievert, P. M. (2012). Immunity to *Staphylococcus aureus* secreted proteins protects rabbits from serious illnesses. *Vaccine*, **30**, 5099–5109.
24. Tkaczyk, C., Hua, L., Varkey, R., Shi, Y., Dettinger, L., Woods, R. *et al.* (2012). Identification of anti-alpha toxin monoclonal antibodies that reduce the severity of *Staphylococcus aureus* dermonecrosis and exhibit a correlation between affinity and potency. *Clin. Vaccine Immunol.* **19**, 377–385.
25. Glanville, J., Zhai, W., Berka, J., Telman, D., Huerta, G., Mehta, G. R. *et al.* (2009). Precise determination of the diversity of a combinatorial antibody library gives insight into the human immunoglobulin repertoire. *Proc. Natl. Acad. Sci. USA*, **106**, 20216–20221.
26. Owyang, A. M., Issafras, H., Corbin, J., Ahluwalia, K., Larsen, P., Pongo, E. *et al.* (2011). XOMA 052, a potent, high-affinity monoclonal antibody for the treatment of IL-1beta-mediated diseases. *MAbs*, **3**, 49–60.
27. Menzies, B. E. & Kernodle, D. S. (1994). Site-directed mutagenesis of the alpha-toxin gene of *Staphylococcus aureus*: role of histidines in toxin activity in vitro and in a murine model. *Infect. Immun.* **62**, 1843–1847.
28. Olson, R., Nariya, H., Yokota, K., Kamio, Y. & Gouaux, E. (1999). Crystal structure of staphylococcal LukF delineates conformational changes accompanying formation of a transmembrane channel. *Nat. Struct. Biol.* **6**, 134–140.
29. Pedelacq, J. D., Maveyraud, L., Prevost, G., Baba-Moussa, L., Gonzalez, A., Courcelle, E. *et al.* (1999). The structure of a *Staphylococcus aureus* leucocidin component (LukF-PV) reveals the fold of the water-soluble species of a family of transmembrane pore-forming toxins. *Structure*, **7**, 277–287.
30. Guillet, V., Roblin, P., Werner, S., Coraiola, M., Menestrina, G., Monteil, H. *et al.* (2004). Crystal structure of leucotoxin S component: new insight into the *Staphylococcus aureus* beta-barrel pore-forming toxins. *J. Biol. Chem.* **279**, 41028–41037.
31. Roblin, P., Guillet, V., Joubert, O., Keller, D., Erard, M., Maveyraud, L. *et al.* (2008). A covalent S-F heterodimer of leucotoxin reveals molecular plasticity of beta-barrel pore-forming toxins. *Proteins*, **71**, 485–496.
32. Yamashita, K., Kawai, Y., Tanaka, Y., Hirano, N., Kaneko, J., Tomita, N. *et al.* (2011). Crystal structure of the octameric pore of staphylococcal gamma-hemolysin reveals the beta-barrel pore formation mechanism by two components. *Proc. Natl. Acad. Sci. USA*, **108**, 17314–17319.
33. Walker, B. & Bayley, H. (1995). Key residues for membrane binding, oligomerization, and pore forming activity of staphylococcal alpha-hemolysin identified by cysteine scanning mutagenesis and targeted chemical modification. *J. Biol. Chem.* **270**, 23065–23071.
34. Inoshima, N., Wang, Y. & Bubeck Wardenburg, J. (2012). Genetic requirement for ADAM10 in severe *Staphylococcus aureus* skin infection. *J. Invest. Dermatol.* **132**, 1513–1516.
35. Kollef, M. H., Shorr, A., Tabak, Y. P., Gupta, V., Liu, L. Z. & Johannes, R. S. (2005). Epidemiology and outcomes of health-care-associated pneumonia: results from a large US database of culture-positive pneumonia. *Chest*, **128**, 3854–3862.
36. Rubinstein, E., Kollef, M. H. & Nathwani, D. (2008). Pneumonia caused by methicillin-resistant *Staphylococcus aureus*. *Clin. Infect. Dis.* **46**, S378–S385.
37. Talan, D. A., Krishnadasan, A., Gorwitz, R. J., Fosheim, G. E., Limbago, B., Albrecht, V. & Moran, G. J. (2011). Comparison of *Staphylococcus aureus* from skin and soft-tissue infections in US emergency department patients, 2004 and 2008. *Clin. Infect. Dis.* **53**, 144–149.
38. King, M. D., Humphrey, B. J., Wang, Y. F., Kourbatova, E. V., Ray, S. M. & Blumberg, H. M. (2006). Emergence of community-acquired methicillin-resistant *Staphylococcus aureus* USA 300 clone as the predominant cause of skin and soft-tissue infections. *Ann. Intern. Med.* **144**, 309–317.
39. Kobayashi, S. D., Malachowa, N., Whitney, A. R., Braughton, K. R., Gardner, D. J., Long, D. *et al.* (2011). Comparative analysis of USA300 virulence determinants in a rabbit model of skin and soft tissue infection. *J. Infect. Dis.* **204**, 937–941.
40. Dryla, A., Prustomersky, S., Gelbmann, D., Hanner, M., Bettinger, E., Kocsis, B. *et al.* (2005). Comparison of antibody repertoires against *Staphylococcus aureus* in healthy individuals and in acutely infected patients. *Clin. Diagn. Lab. Immunol.* **12**, 387–398.
41. Kluytmans, J., van Belkum, A. & Verbrugh, H. (1997). Nasal carriage of *Staphylococcus aureus*: epidemiology, underlying mechanisms, and associated risks. *Clin. Microbiol. Rev.* **10**, 505–520.
42. Verkaik, N. J., de Vogel, C. P., Boelens, H. A., Grumann, D., Hoogenboezem, T., Vink, C. *et al.* (2009). Anti-staphylococcal humoral immune response in persistent nasal carriers and noncarriers of *Staphylococcus aureus*. *J. Infect. Dis.* **199**, 625–632.
43. Wertheim, H. F., Vos, M. C., Ott, A., van Belkum, A., Voss, A., Kluytmans, J. A. *et al.* (2004). Risk and outcome of nosocomial *Staphylococcus aureus* bacteraemia in nasal carriers versus non-carriers. *Lancet*, **364**, 703–705.
44. Adhikari, R. P., Ajao, A. O., Aman, M. J., Karauzum, H., Sarwar, J., Lydecker, A. D. *et al.* (2012). Lower antibody levels to *Staphylococcus aureus* exotoxins are associated with sepsis in hospitalized adults with invasive *S. aureus* infections. *J. Infect. Dis.* **206**, 915–923.
45. Hawkins, J., Kodali, S., Matsuka, Y. V., McNeil, L. K., Mininni, T., Scully, I. L. *et al.* (2012). A recombinant Clumping factor A containing vaccine induces functional antibodies to *Staphylococcus aureus* that are not observed after natural exposure. *Clin. Vaccine Immunol.* **19**, 1641–1650.
46. Shorr, A. F., Tabak, Y. P., Gupta, V., Johannes, R. S., Liu, L. Z. & Kollef, M. H. (2006). Morbidity and cost

- burden of methicillin-resistant *Staphylococcus aureus* in early onset ventilator-associated pneumonia. *Crit. Care*, **10**, R97.
47. Marks, J. D. & Bradbury, A. (2004). Selection of human antibodies from phage display libraries. *Methods Mol. Biol.* **248**, 161–176.
 48. Hildebrand, A., Pohl, M. & Bhakdi, S. (1991). *Staphylococcus aureus* alpha-toxin. Dual mechanism of binding to target cells. *J. Biol. Chem.* **266**, 17195–17200.
 49. Otwinowski, Z. & Minor, W. (1997). Processing of X-ray diffraction data. *Methods Enzymol.* **276**, 307–326.
 50. McCoy, A. J., Grosse-Kunstleve, R. W., Storoni, L. C. & Read, R. J. (2005). Likelihood-enhanced fast translation functions. *Acta Crystallogr., Sect. D: Biol. Crystallogr.* **61**, 458–464.
 51. Emsley, P. & Cowtan, K. (2004). Coot: model-building tools for molecular graphics. *Acta Crystallogr., Sect. D: Biol. Crystallogr.* **60**, 2126–2132.
 52. Murshudov, G. N., Vagin, A. A. & Dodson, E. J. (1997). Refinement of macromolecular structures by the maximum-likelihood method. *Acta Crystallogr., Sect. D: Biol. Crystallogr.* **53**, 240–255.
 53. Briggs, P. (2000). http://www.ccp4.ac.uk/newsletters/newsletter38/03_surfarea.html. *CCP4 Newsletter 2*.